Analyst

PAPER

View Article Online
View Journal | View Issue

Check for updates

Cite this: *Analyst*, 2018, **143**, 4630

Size-dependent adsorption and its application in determining the number of surfactant molecule adsorbed on multimodal SiO_2 particles by 2D-DCS†

Guolan Tian, Lan Chen,* Renxiao Liu and Guanglu Ge*

Received 10th June 2018,
Accepted 11th August 2018

DOI: 10.1039/c8an01068d

rsc.li/analyst

Quantitative analysis using surfactant–particles interaction is the basis for many applications. *In situ* measurements of surfactant adsorption on nanoparticles are important to understanding adsorption kinetics. However, it is quite difficult to determine the individual numbers for each monomodal particles in a multimodal mixture system by current technologies. To cope with this problem, a new method, *i.e.* 2D differential centrifugal sedimentation (2D-DCS), has been developed and applied *in situ* to measure the number of CTAB molecules adsorbed on the surface of silica particles, assuming that the adlayer is composed of a compact CTAB monolayer. Results show that 2D-DCS can measure the adsorption amount for particles not only with single size distribution but also with multiple size distributions. The number of adsorbed CTAB per nm^2 on silica particles determined by 2D-DCS are 1.4 and 3.9 for the monomodal particles of 210 and 1000 nm, respectively, which is similar to that measured by ζ-potential, DLS and UV-vis spectrometry, and 1.4, 2.3 and 2.5 for 210, 430 and 700 nm particles, respectively, for a trimodal particle system, where the size-dependent adsorption is difficult to be simultaneously measured by other technologies.

Introduction

As one of the most common nanomaterials, SiO_2 nanoparticles (NPs) are widely used in cosmetics, food, varnishes, papermaking, and drugs.[1] Understanding the mechanism of surfactant adsorption onto the silica-liquid interfaces benefits many applications including detergency, lubrication, wetting, stabilization of solid dispersions, selective flotation of minerals, and protection of metal surfaces.[2–6] In the past several decades, the interaction between ionic surfactants and silica particles in many industrial products and processes has been extensively studied.[7–17]

Since the surfaces of the silica particles synthesized by numerous methods are usually negatively charged, cationic surfactant *e.g.* CTAB (cetyltrimethylammonium bromide) can be used as probe molecule to investigate the interaction between the particles and surfactant. Neutralizing the surfaces of the negatively charged SiO_2 particles with different amounts of CTAB can tune the particle aggregate size and can also aid to understand the SiO_2 particles–CTAB interaction mechanism in a quantitative manner.[18]

Traditionally, qualitative measurement of the amount of surfactant adsorbed at solid–liquid interfaces is usually carried out by contact angle or electrokinetic measurements.[19] Later on, several other experimental methods such as spectroscopy, surface force measurements, calorimetry, nuclear magnetic resonance (NMR) spectroscopy, ellipsometry, fluorescence decay, and neutron reflectometry have been used to study the surfactant–particle interaction mechanism.[17]

However, quantitative analysis on the interaction between SiO_2 NPs and surfactants are not well-developed and are mostly carried out by zeta-potential titration/dynamic light scattering (DLS), where its isoelectric point (IEP) is monitored and determined by sharp change in the surface charge from negative to positive. Moreover, the particles aggregate due to their neutralization accompanied by the decrease in turbidity of the colloidal solution, which can be recorded by UV-vis spectrometer. Adsorption of CTAB on a smooth SiO_2 film has been investigated by ellipsometry and the result is in agree-

CAS Key Laboratory of Standardization and Measurement for Nanotechnology, CAS Center for Excellence in Nanoscience, National Center for Nanoscience and Technology, No. 11 ZhongguancunBeiyitiao, Beijing 100190, China. E-mail: chenlan@nanoctr.cn, gegl@nanoctr.cn; Tel: +86 10 82545556

†Electronic supplementary information (ESI) available: Additional information including synthesized SiO_2 nanoparticles by SEM, layer thickness of CTAB Sorption on SiO_2 nanoparticles by TEM, 2D size distribution for CTAB adsorbed on monomodal and multimodal SiO_2 particles measured by DCS, s ζ-potential measurement on the titration of CTAB-to SiO_2 NPs, spectroscopic of the adsorbed CTA^+ on SiO_2 nanoparticles by FTIR as shown in Fig. S1–S6 and Table S1. See DOI: 10.1039/c8an01068d

ment with a two-step adsorption model including monolayer and bilayer adsorption occurring in the CTAB solution with different concentrations.[3] The thickness of the adsorbed compact CTAB monolayer, *i.e.* adlayer, was measured to be 2.6 nm.

As expected, CTA^+ ion is strongly adsorbed on the surface of the negatively charged SiO_2 particles due to electrostatic interactions. The *in situ* FT-IR/IRS adsorption density equation has been successfully used to determine adsorption density of the CTAB micelles at silica surface. When the solution concentration is 1 mM, the calculated FTIR/IRS adsorption density (3.6 mmol m^{-2}, ~2.2 CTAB per nm^2) is in close agreement with that measured from fast Fourier transform (FFT) quantitative analysis imaged by soft contact AFM on spherical CTAB micelles (3.2 mmol m^{-2}, ~1.9 CTAB per nm^2).[17] The adsorption density reaches its maximum capacity or plateau at ~0.24 mmol g^- (~5.5 CTAB per nm^2) suggesting the formation of bilayered micelles.[1]

Though these technologies can be used to determine the adsorption of CTAB onto the nanoparticles, it is impossible to differentiate size-dependent adsorption for particle suspension with multiple sized distributions. Recently, Dawson *et al.* employed differential centrifugal sedimentation (DCS) to study biomolecule–nanoparticle interaction by comparing the difference in the diameter of gold nanoparticles obtained before and after the formation of the protein corona.[20] This indicates that DCS can be used to monitor and analyse protein–particle interaction caused by the change in pH, ionic strength or addition of the surfactant. Moreover, the size-resolving capability of DCS can be used to monitor protein partitioning on nanoparticle surfaces of multiple sized system, which provides important information about particle–protein interactions under competitive conditions.[21]

Consequently, this study primarily aims at a better understanding on the interaction between the SiO_2 nanoparticles and the surfactant, and the conformational arrangement of its adlayer using CTAB as probe molecules. The SiO_2 NPs used here are highly uniform and negatively charged with monomodal or multimodal distributions, which provide a comparable base to quantitatively measure the adsorption of CTAB molecules on these particles. With an increase in CTAB molecules, mono- or bi-layered surfactant adlayer can be formed on the surface of the SiO_2 NPs accompanied by subsequent particle aggregation and re-dispersion. Comparatively, the aggregation behaviour of the monomodal nanoparticle has been parallelly investigated by DLS, zeta-potential measurements and UV-vis absorbance spectroscopy, where the IEP or cloud point (CP) has been detected to determine the maximum adsorption amount for formation of a compact CTAB monolayer. However, all of these techniques can only obtain an averaged adsorption amount for a multimodal system and cannot separate individual IEP or CP of each monomodal particle from the others. Herein, a new method, namely, two dimensional (2D) differential centrifugal sedimentation has been developed and used to quantitatively analyse the surfactant–nanoparticle interaction in a multimodal system and synchronously determine the monolayer adsorption amount separately for each particle size. Similar technology has been used by Peukert *et al.* in analytical ultracentrifugation (AUC) to discriminate minute differences between the polydisperse core–shell QDs, which shows very high resolution and reliability in determining the size and effective density of these nanoparticles through 2D-AUC.[22]

Experimental

Materials

Tetraethyl orthosilicate (TEOS, ≥99%) and CTAB (≥99%) were purchased from Aladdin. Acetone (HPLC, GC) was obtained from Beijing Chemical Reagent Inc. and NH_3 (7 mol L^{-1} in MeOH) was purchased from Sam Chemical Technology (Shanghai) Co., Ltd. All chemicals were used as received. Deionized water with resistivity of 18.2 MΩ cm was obtained from a Millipore ultrapure water system.

SiO_2 nanoparticle synthesis

Monodispersed SiO_2 nanoparticles were prepared by hydrolysis of TEOS in an acetone medium in the presence of appropriate amount of water and anhydrous ammonia methanol solution. For a typical preparation, two solutions with equal volume were rapidly mixed under vigorous stirring. One solution contained acetone and TEOS and the other composed acetone, water, and anhydrous ammonia. The mixture was further stirred for 1–3 hours and aged in an oven at 60 °C for 3–7 hours. The resultant precipitate was collected by centrifugation and subsequently washed with acetone and DI water 3 times. The as-received wet product was dried under vacuum at 60 °C for ~10 hours. SiO_2 particles with tunable size in the range of 200 to 1000 nm were obtained by adjusting the ratios of water to TEOS and ammonia to TEOS.

Analysis and measurement

The particle–surfactant is considered to interact *via* coulombic forces between CTA^+ and negatively charged silica particles (Scheme 1) and its measurements were carried out by differential centrifugal sedimentation (DCS, Model DC24000 UHR CPS Instruments, Inc.) equipped with a high speed centrifugation

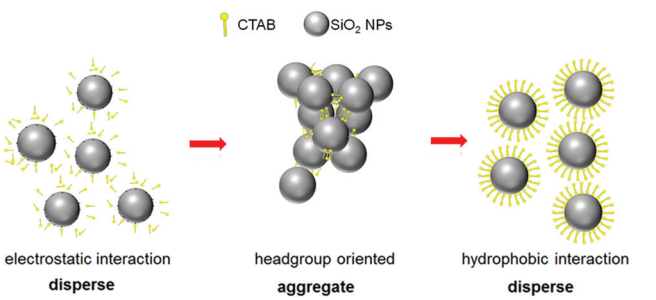

Scheme 1 Model for CTAB adsorption onto silica particles in aqueous solution.

motor (up to 24 000 rpm) and an optical detector with a detectable size limit of 10 nm, to obtain time/space-dependent parameters such as size and density. Furthermore, ζ-potential and turbidity titration of SiO_2 colloids by CTAB were measured by DLS (Malvern Zetasizer Nano ZS instrument) and UV-visible spectrometer (PerkinElmer Lambda 650, λ_{ab} = 407 nm), respectively, where the IEP can be determined by the sharp change in the ζ-potential from negative to positive and the cloud point, or "clear" point in this case, can be determined by the sharp decline in the UV-vis absorbance of the solution. SiO_2 particles were directly imaged using a ZEISS Merlin (Germany) scanning electron microscope (SEM) operated at an accelerating voltage of 5 kV. For IR spectral analysis, a wet SiO_2 colloid sample collected from the colloidal suspension was dropped on the ZnSe crystal substrate and dried to form a particle film. The IR spectra of surfactant-adsorbed SiO_2 particles were recorded at 4 cm^{-1} resolution by a NICOLET FTIR iS50 spectrometer mounted with a DTGS detector.

Results and discussion

Characterization of silica nanoparticles

SEM images show spherical morphology and uniform size for the bare silica particles in Fig. S1 (see ESI†). In order to observe the CTAB adlayer directly, CTAB-adsorbed SiO_2 nanoparticles were taken out from the solution, dropped onto the TEM grid and dried under infrared light. As seen in Fig. 1, the silica particle is coated with a layer of lighter matter at an average thickness of 6.7 ± 1.4 nm (Median 6.445), which is roughly two times larger than that of the CTAB monolayer, and further details can be found in Fig. S2 and Table S1 (see ESI†).

Interaction of CTAB–SiO_2 nanoparticles with monomodal size distributions

2D-DCS is developed and used to monitor and measure the IEP of SiO_2 nanoparticles in the solution titrated by CTAB, which can determine the number of probe molecules, *i.e.* CTAB per nm^2, on surface of the particles. Without CTAB addition, silica particles are well dispersed in water with an average particle diameter of 210 nm while the adsorption of CTA^+ ions results in the destabilization of silica dispersion (Fig. S3, see ESI†). For spherical particle, its sedimentation coefficient (s) can be calculated by Stokes law based on the drag-centrifugal force balance and expressed as

$$s = \frac{\ln(R_D/R_0)}{\omega^2 t} = \frac{{d_{sd}}^2(\rho_{sd} - \rho_f)t_{sd}}{18\eta t} \quad (1)$$

where d_{sd}, ρ_{sd} and t_{sd} are diameter, density and movement time of the reference particle, respectively; ρ_f and η are density and average viscosity of the fluid, respectively, at the measurement temperature; ω, R_0 and R_D are rotation speed of the disc, radial distance of the liquid surface and distance of the detection place to the center of the disc, respectively.[23] The reference SiO_2 nanoparticles with d_{sd} = 0.15 μm and ρ_{sd} = 2.16 g cm^{-3} were measured in sucrose solution with an average density of ρ_f = 1.064 g cm^{-3} and average viscosity of η = 1.1 cP (30 ± 1 °C). In a typical measurement, more than 20 titrations with incremental ratios of CTAB to SiO_2 (RCtS) were gradually measured by DCS, and the corresponding time-resolved absorbance curves obtained were normalized. Then, the sedimentation coefficient (s) for each curve was obtained based on the drag-centrifugal force balance calculated using the above equation. Finally, 2D contours were plotted by overlapping all these titration curves together in Origin, where color denotes the absorbance intensity while x and y axes denote settlement coefficient and concentration of CTAB in the titration, respectively.

As seen in Fig. 2, 2D sedimentation coefficient (s) distribution clearly shows that the absorbance intensity changes with both CTAB concentration and sedimentation coefficient. When the ratio of CTAB to SiO_2 is below ~0.03 mmol g^{-1} (*i.e.* 1.4 CTAB molecules per nm^2 SiO_2 particle surface), the nominal colloid particle size measured gradually increases with an increase in CTAB concentration. The largest s, which corresponds to the biggest aggregate formed by particle coagulation in solution and the number of CTAB adsorbed nm^{-2} on the particle surfaces are 7.0 × 10^{-8} s and 1.4, respectively. A further increase in CTAB concentration results in dispersion of the aggregates; the RCtS determined by DCS is almost same to that measured by ζ-potential and the corresponding SEM images show that the CTAB-adsorbed SiO_2 nanoparticles change with the ζ-potential titration (Fig. 3).

As seen in Fig. 3, ζ-potential of the silica particles gradually increases from −47 to +37 mV with the titration against CTAB molecules. The isoelectric point is obtained at ~1.6 nm^{-2} of RCtS, which implies that the charge per nm^2 of silica surface is completely neutralized by 1.6 CTAB molecules (Fig. 3(a)). However, SEM images show different morphologies at different stages of the titration, *e.g.* a well-dispersed phase is observed at the starting-point while slight and significant agglomeration causes broad distributions at points A and B, respectively. Coagulation is seen at point C when the ζ-potential approaches zero and is confirmed by the formation of more fibrous surfaces. Aggregates start to disperse when the ζ-potential crosses zero and approaches positive value upon further addition of CTAB molecules at point D. Eventually, these aggregates are totally dispersed at stages E and F with more positive surface charge, where the formation of a

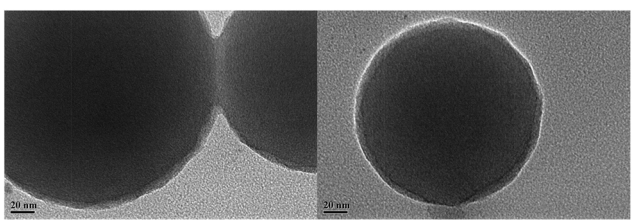

Fig. 1 TEM images of CTAB-adsorbed on SiO_2 nanoparticles (160 ± 10 nm).

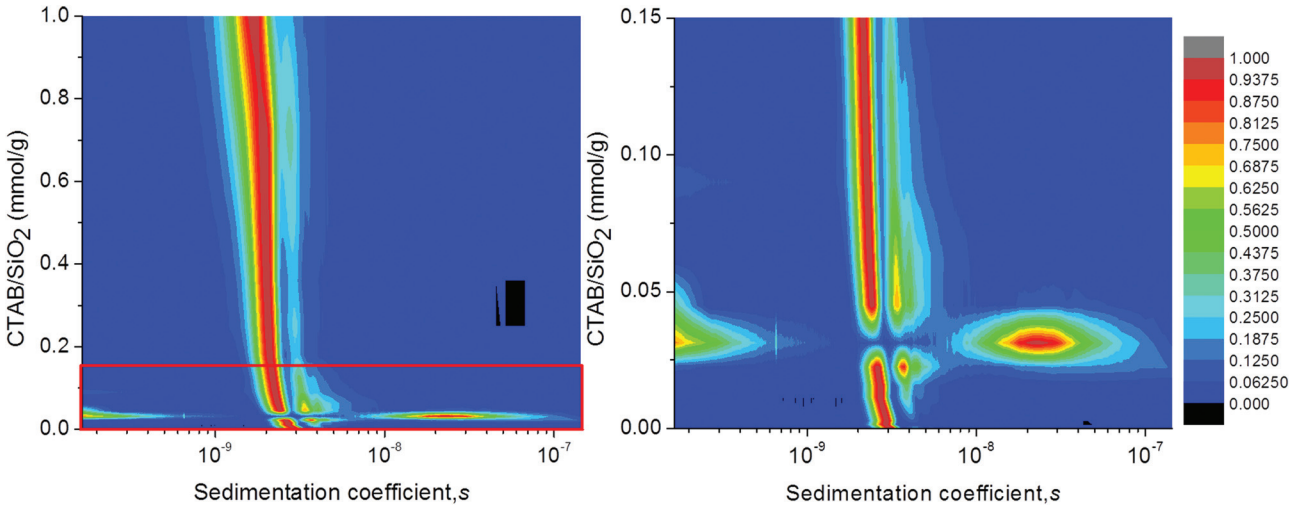

Fig. 2 2D sedimentation coefficient distribution for CTAB-adsorbed SiO_2 particles (210 nm) measured by 2D-DCS.

compact CTAB bilayer on the particles renders SEM images blurry than that of the others. This particle aggregation and dispersion caused by increasing CTAB concentration can be attributed to the formation of a monolayer (hemimicelle) and a bilayer (micelle) of the CTAB molecules on the particles, respectively, as depicted in Scheme 1.

Similarly, the same tendency is observed by DLS and UV-vis spectrometry, where adsorption of CTA^+ ions results in destabilization and re-stabilization of the silica dispersion (Fig. 4(a)). When the RCtS is below ~0.009 mmol g^{-1} (*i.e.* 1.96 CTAB molecules per nm^2 SiO_2 particle surface), the nominal colloid particle size measured by DLS gradually increases with an increase in CTAB concentration. Between 0.009–0.036 mmol g^{-1}, a drastic increase in the particle size is observed. A further increase in CTAB concentration above 0.036 mmol g^{-1} (7.84 CTAB per nm^2) results in decrease of the overall particle size and dispersion of the aggregates. DLS analysis shows that the sizes of majority of colloidal particles are about 1000 nm. Meanwhile, ζ-potential of SiO_2 colloids increases from −77 mV with an increase in CTAB concentration. The isoelectric point is obtained at 0.02 mmol g^{-1} (~4.3 nm^{-2}) of RCtS implying the surface charge is completely neutralized by CTAB molecules (Fig. 4(a)). The ζ-potential increases from −77 mV and crosses zero line at a point when a sharp increase in the diameter of particles (aggregates) occurs with the titration of CTAB against SiO_2. Eventually, ζ-potential of the particle suspension reaches +70 mV on titration against excess CTAB, and the diameter of particles (aggregates) decreases dramatically until it reaches to that of bare SiO_2 particles, which indicates complete dispersion of the silica aggregates.

As seen in Fig. 4(b), particle aggregation can also be detected by UV-vis spectrometry based on turbidity changes. Absorbance caused by CTAB is negligible compared with that caused by particles. An obvious decrease in turbidity can be seen at RCtS of 0.018 mmol g^{-1} (~3.9 nm^{-2}) upon addition of CTAB, which is recovered after the equivalent number concentration of CTAB reaches ~0.055 mmol g^{-1} (~12 nm^{-2}) as seen in Fig. 4(b). To further verify whether any free surfactant is present in the solution when very low concentrations of CTAB is used, the SiO_2–CTAB mixture undergoes centrifugal ultrafiltration at 7000 rpm using a membrane with a nominal molecular weight limit of 10 kDa (Millipore) and is measured by ζ-potential. As seen in Fig. S4,† ζ-potential of the SiO_2–CTAB mixture gradually increases from −48 mV to +47 mV with titration against CTAB molecules. The isoelectric point is obtained at ~0.025 mmol L^{-1} (~0.05 mmol g^{-1} of RCtS), which implies that the surface charge of particles is completely neutralized by CTAB molecules while ζ-potential of the supernatant, collected by ultrafiltration, is largely kept zero or slight negative, which indicates no free CTAB molecules are present in the solution below this RCtS. Even when the ratio of CTAB to SiO_2 NPs reaches 0.15 mmol g^{-1} (~0.075 mmol L^{-1}), *i.e.* the titration point, which implies all the available SiO_2 NP surfaces are completely adsorbed with CTAB molecules, the ζ-potential of the supernatant is still below zero. ζ-Potential of the pure CTAB solution (Fig. 4S,† red curve) increases with the increase in the CTAB concentration, and is significantly greater than that of the supernatant filtered by centrifugal ultrafiltration (Fig. 4S,† blue curve). As a result, all CTAB molecules in the solution are completely adsorbed onto the surface of SiO_2 NPs before the titration point (0.15 mmol g^{-1}), whereas, free CTAB molecules exist in the solution only if excess CTAB are used to titrate the SiO_2 NPs (>0.15 mmol g^{-1}). Moreover, the adsorption of CTAB onto SiO_2 surface makes its ζ-potential further positive than its pure CTAB counterpart indicating that the negative silica surface can enrich the positive surfactant molecules. It confirms that DCS can be used to quantitatively investigate the surfactant–particle interactions with similar performance as ζ-potential and UV-vis spectrometry. The results show that the number of CTAB determined by 2D-DCS is quite close to those measured by ζ-potential and UV-vis spectrometry, as seen in Table 1.

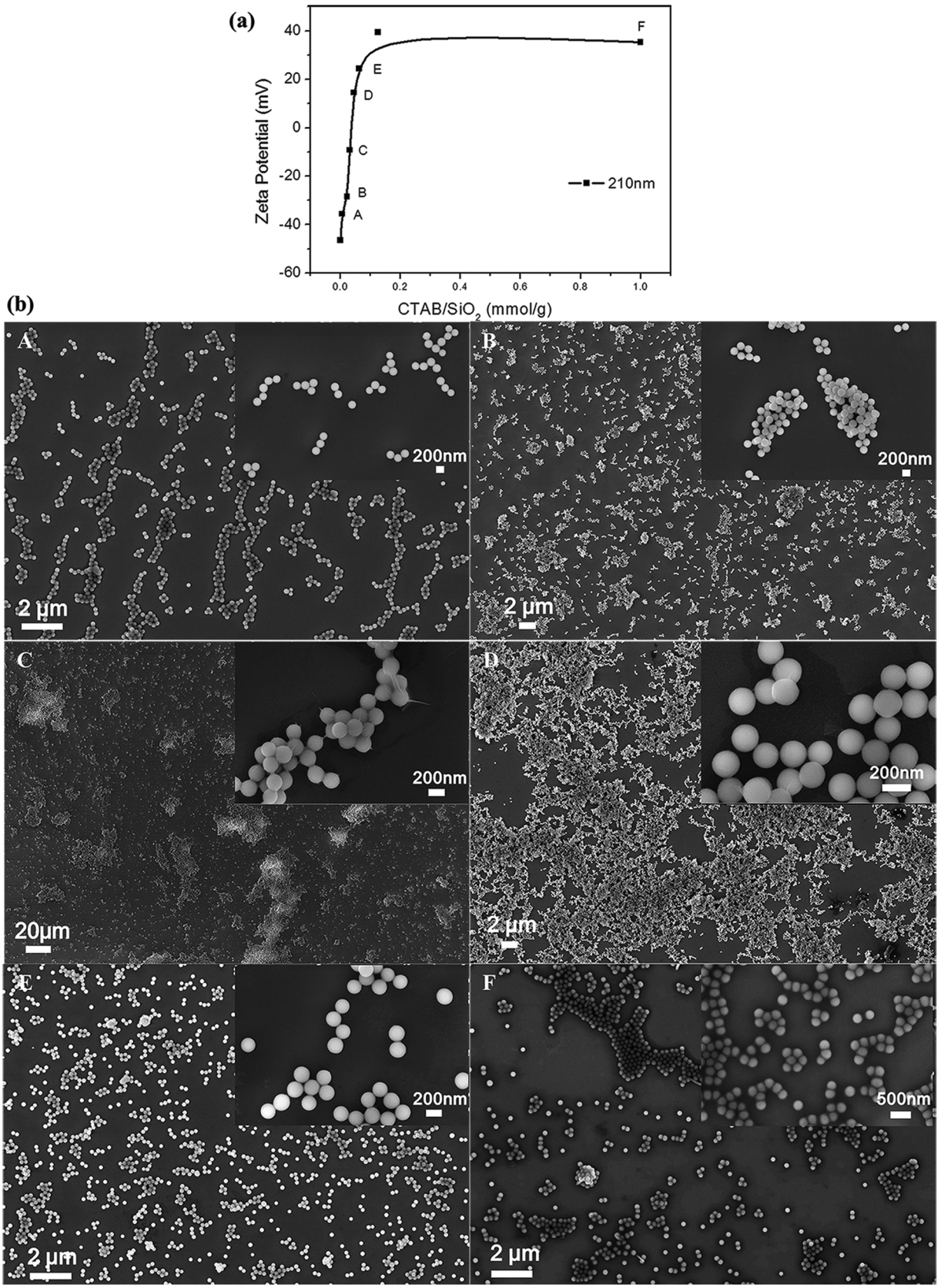

Fig. 3 ζ-Potential measurements (a) of CTAB–SiO_2 interaction (210 nm, top panel) and corresponding SEM images (b) of CTAB-adsorbed SiO_2 nanoparticles at different phases of titration as shown on the curve in (a).

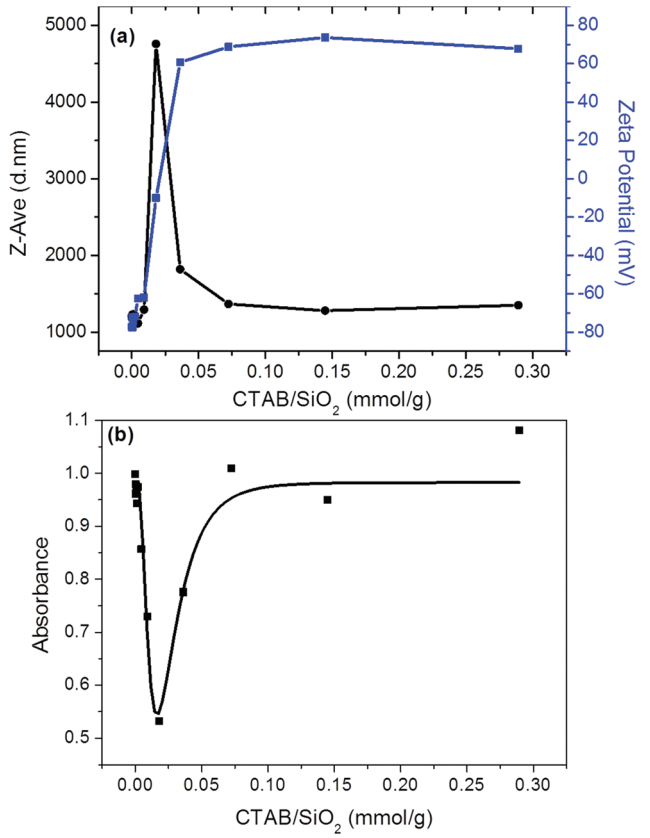

Fig. 4 DLS/ζ-potentials measurements (a) and turbidity measurements by UV-visible spectrometry at 407 nm (b) of CTAB–SiO_2 (1000 nm) interaction.

Table 1 The number of CTAB per nm^2 adsorbed on the surface of SiO_2 particles measured by various techniques

	CTAB/SiO_2		
	210 nm	1000 nm	210 + 430 + 700 nm
DCS	1.4	3.9	1.4, 2.3, 2.5 (average 2.4)
DLS	1.4	3.9	—
ζ-Potential	1.6	4.3	2.02
UV-vis	—	3.9	—

The structural arrangements and conformations of the adsorbed CTAB on SiO_2 nanoparticles are then analyzed by FTIR in Fig. S5 (see ESI†). For pure SiO_2 nanoparticles (Fig. S5(b)†), FTIR spectrum in the 3800–2500 cm^{-1} range exhibits a characteristic broad peak centered at 3369 cm^{-1} and can be assigned to the O–H stretching vibrations of the surface hydroxyls and water.[24] Two shoulder bands at 3622 and 3727 cm^{-1} may be assigned to the O–H stretching mode of isolated surface silanol groups. In the 2000–800 cm^{-1} region, there are a series of absorption bands related to Si–O vibrations, of which the strongest is at 1081 cm^{-1} with a shoulder around 1230 cm^{-1}, which is due to the asymmetric Si–O stretching mode of Si–O–Si bridge bonds in the skeleton. Bands with medium intensities at 941 and 799 cm^{-1} are associated with stretching vibrations of surface Si–O bonds. For CTAB-adsorbed silica nanoparticles (Fig. S5(c)†), the following characteristic absorption bands are observed: C–H stretching modes in 3000–2800 cm^{-1}, CH_2 bending and CH_3–(N^+) deformation modes in 1500–1450 cm^{-1} range.[25,26] Additionally, in presence of CTAB, the O–H stretching vibration band at 3369 cm^{-1} significantly shifts to a lower frequency and broadens, and the surface Si–O vibration bands at 1081, 944 and 803 cm^{-1} also shifts several wavenumbers, indicating strong interactions between CTAB and SiO_2 surfaces. The spectral information gives unambiguous evidence of the CTAB adsorption on SiO_2 nanoparticles, even after washing (Fig. S5(d)†).

Interaction of CTAB–SiO_2 nanoparticles with trimodal size distributions

The highlight feature of 2D-DCS is that it not only measures particles with single size distributions but also tracks and measures particle system with multiple size distributions simultaneously, for example, 210, 430 and 700 nm trimodal particle mixture used in this study. For this multimodal particle mixture, sedimentation coefficient distribution for different particle sizes can be separately determined by 2D-DCS as seen in Fig. S6 (see ESI†). However, IEP or CP determined in such multimodal particle mixture by ζ-potential and UV-vis spectrometry cannot differentiate size-dependent adsorption. As seen in Fig. 5, three well-defined sedimentation coefficient distributions are obtained for 210, 430 and 700 nm particles by 2D-DCS in simultaneously. The sudden change point determined by the measurement is slightly different, *i.e.* 1.4, 2.3 and 2.5 CTAB per nm^2 (~0.03 mmol g^{-1}) for 210, 430 and 700 nm particles, respectively. These are slightly lower than the molecular surface density of CTAB hemimicelles due to formation of loose 'micelles' around a solid core with larger curvature compared to soft micelles comprising only CTAB molecules. As seen in Table 1, RCtS obtained by 2D-DCS is almost same as those determined by other technologies such as DLS, ζ-potential and UV-vis spectrometry for the monomodal particles of 210 and 1000 nm. In the multimodal mixture, other techniques can only provide an average RCtS for all three particle sizes based on their total surface area whereas, 2D-DCS can provide size-dependent adsorption data for different particle sizes besides the averaged one.

Furthermore, adsorption of CTAB to SiO_2 is confirmed to be size-dependent, *i.e.* curvature-related in a multimodal particle suspension and a linear regression can be obtained when fitting the number of CTAB molecules adsorbed on SiO_2 particle surfaces against square of the curvature (k^2) of these particles, which is equal to the reciprocal square of the particle diameter ($1d^{-2}$) as seen in Fig. 6. Alternatively, the flatter the particle surface, the more compact and denser the surfactant monolayer formed. Maximum surface RCtS is 2.6 nm^{-2} obtained at a curvature of 0 ($k = 0$), *i.e.* on a flat surface according to the extrapolated results. Calculated cross sectional area for the CTAB head group is 0.385 nm^2 at zero curvature ($k = 0$), which is smaller than that reported by Hamilton *et al.*

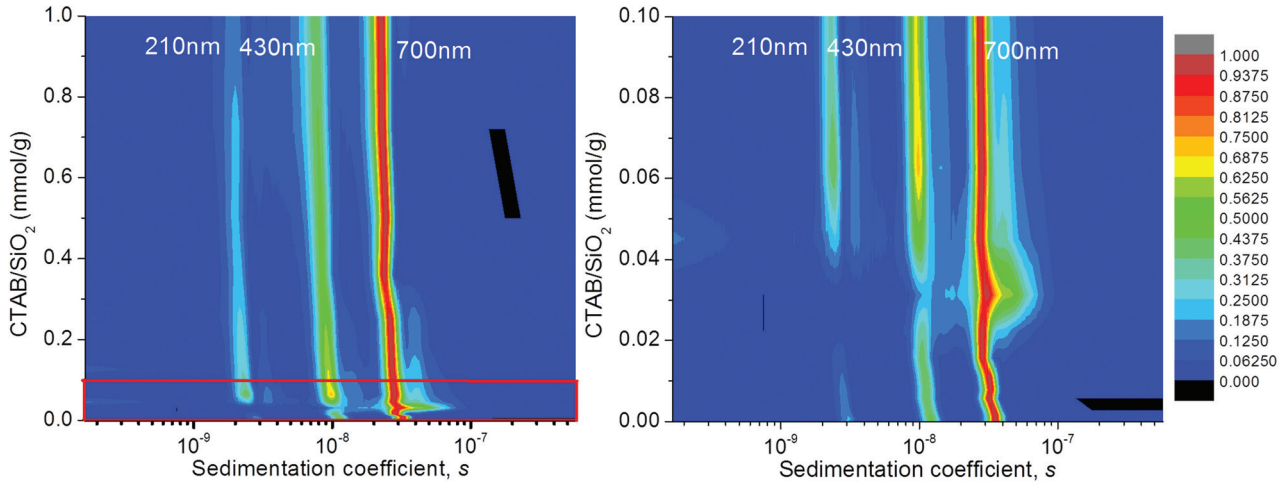

Fig. 5 2D sedimentation coefficient distributions for CTAB adsorbed SiO_2 particles with multiple size distributions of 210, 430 and 700 nm measured by 2D-DCS.

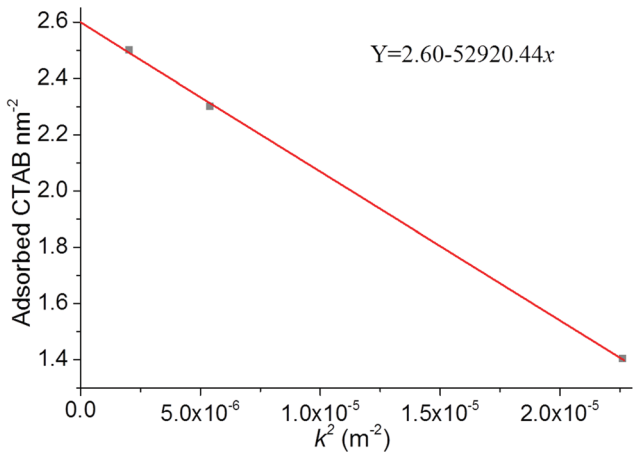

Fig. 6 Relationship between CTAB molecule number adsorbed per nm^2 particle surface and square of the curvature (k^2) of particle.

(0.59 nm^2)[1] and Gharibi *et al.* (0.657 nm^2)[27] for a monolayer formed at the water/air interface while larger than that measured by BET method (0.32 nm^2) in dry state.[1] However, the cross section area of CTAB head group at critical micelle concentration is determined as 0.39 nm^{-2} due to the formation of more compact micelles comparable to that adsorbed on a flat surface as calculated in this study.[28]

Conclusions

In this work, DCS is used for the first time to measure the surfactant–nanoparticle interaction, *i.e.* CTAB adsorption on SiO_2 particles of different size. Here, CTAB molecules act as both flocculant and probe molecules to precipitate the particles and quantify their adsorption on surfaces of the particles, respectively. This study demonstrates that DCS can provide two dimensional information on the particle size distribution varying with both the amount of surfactant and the size of particles (or aggregates). 2D-DCS is a very convenient technology to correlate the adsorbed amount of surfactant and the aggregate (or single particle) size. Experimental results show that 2D-DCS can measure not only the adsorption on the particles with monomodal distribution but also those with multimodal distribution, which is difficult to measure simultaneously using other technologies. Surface RCtS is determined at 1.4 and 3.9 for monomodal particle systems of 210 and 1000 nm, respectively, which is similar to that measured by DLS, ζ-potential and UV-vis spectrometry. RCtS of 1.4, 2.3 and 2.5 were measured for a trimodal particle system composed of 210, 430 and 700 nm particles, which cannot be simultaneously measured by other technologies.

Conflicts of interest

There are no conflicts to declare.

Acknowledgements

The authors thank the Ministry of Science and Technology (No. 2016YFA0200904), the National Key Research and Development Program of China (No. 2016YFA0200904) and the Strategic Priority Research Program of CAS (No. XDA09040400) for the financial supports.

References

1 W. Wang, B. H. Gu, L. Y. Liang and W. A. Hamilton, *J. Phys. Chem. B*, 2004, **108**, 17477–17483.
2 K. Esumi, *J. Colloid Interface Sci.*, 2001, **241**, 1–17.
3 Z. C. Bi, W. S. Liao and L. Q. Qi, *Appl. Surf. Sci.*, 2004, **221**, 25–31.

4 F. Venditti, A. Ceglie, G. Palazzo, G. Colafemmina and F. Lopez, *J. Colloid Interface Sci.*, 2007, **310**, 353–361.
5 X. Xin, H. Zhang, G. Xu, Y. Tan, J. Zhang and X. Lv, *Colloids Surf., A*, 2013, **418**, 60–67.
6 Y. Liu, M. Tourbin, S. Lachaize and P. Guiraud, *Chemosphere*, 2013, **92**, 681–687.
7 V. Monticone and C. Treiner, *J. Colloid Interface Sci.*, 1994, **166**, 394–403.
8 B. Kitiyanan, J. H. Ohaver, J. H. Harwell and S. Osuwan, *Langmuir*, 1996, **12**, 2162–2168.
9 K. Esumi, H. Mizutani, K. Shoji, M. Miyazaki, K. Torigoe, T. Yoshimura, Y. Koide and H. Shosenji, *J. Colloid Interface Sci.*, 1999, **220**, 170–173.
10 M. Drach, A. Andrzejewska and J. Narkiewicz-Michalek, *Appl. Surf. Sci.*, 2005, **252**, 730–744.
11 E. Tyrode, M. W. Rutland and C. D. Bain, *J. Am. Chem. Soc.*, 2008, **130**, 17434–17445.
12 W. Jiang, K. Yang, R. W. Vachet and B. Xing, *Langmuir*, 2010, **26**, 18071–18077.
13 C.-K. Yang, *Comput. Phys. Commun.*, 2011, **182**, 39–42.
14 L. Liggieri, E. Santini, E. Guzman, A. Maestro and F. Ravera, *Soft Matter*, 2011, **7**, 7699–7709.
15 E. Santini, J. Kragel, F. Ravera, L. Liggieri and R. Miller, *Colloid Surf., A*, 2011, **382**, 186–191.
16 L. Jiang, S. Li, W. Yu, J. Wang, Q. Sun and Z. Li, *Colloid Surf., A*, 2016, **488**, 20–27.
17 V. K. Paruchuri, K. Q. Fa, B. M. Moudgil and J. D. Miller, *Appl. Spectrosc.*, 2005, **59**, 668–672.
18 B. Fouconnier, A. Roman-Guerrero and E. Jaime Vernon-Carter, *Colloid Surf., A*, 2012, **400**, 10–17.
19 D. W. Fuerstenau, T. W. Healy and P. Somasundaran, *Trans. Soc. Min. Eng. AIME*, 1964, **229**, 321–324.
20 P. M. Kelly, C. Åberg, E. Polo, A. O'Connell, J. Cookman, J. Fallon, Ž. Krpetic and K. A. Dawson, *Nat. Nanotechnol.*, 2015, **10**, 472–479.
21 R. Wang, L. Chen, D. Li, R. Liu and G. Ge, *Part. Part. Syst. Charact.*, 2017, **34**(12), 1700134.
22 J. Walter, G. Gorbet, T. Akdas, D. Segets, B. Demeler and W. Peukert, *Analyst*, 2017, **142**, 206–217.
23 R. Wang, Y. Ji, X. Wu, R. Liu, L. Chen and G. Ge, *RSC Adv.*, 2016, **6**, 43496–43500.
24 C. M. Koretsky, D. A. Sverjensky, J. W. Salisbury and D. M. Daria, *Geochim. Cosmochim. Acta*, 1997, **61**, 2193–2210.
25 W. Wang, L. M. Li and S. Q. Xi, *J. Colloid Interface Sci.*, 1993, **155**, 369–373.
26 W. Wang, L. Li and S. Xi, *Chin. J. Chem. Phys.*, 1993, **6**, 553–558.
27 B. Sohrabi, H. Gharibi, B. Tajik, S. Javadian and M. Hashemianzadeh, *J. Phys. Chem. B*, 2008, **112**, 14869–14876.
28 M. A. Rodriguez, M. Munoz, M. D. Graciani, M. S. F. Pachon and M. L. Moya, *Colloid Surf., A*, 2007, **298**, 177–185.